

# How to Handle Irregular Distribution of SPH Particles in Dynamic Fracture Analysis

MARTIN HUŠEK, JIŘÍ KALA, FILIP HOKEŠ, PETR KRÁL  
Faculty of Civil Engineering, Institute of Structural Mechanics

Brno University of Technology

Veveří 331/95, 602 00 Brno

CZECH REPUBLIC

[husek.m@fce.vutbr.cz](mailto:husek.m@fce.vutbr.cz), [kala.j@fce.vutbr.cz](mailto:kala.j@fce.vutbr.cz), [hokes.f@fce.vutbr.cz](mailto:hokes.f@fce.vutbr.cz), [kral.p@fce.vutbr.cz](mailto:kral.p@fce.vutbr.cz),

<http://www.fce.vutbr.cz>

*Abstract:* The failure of quasi-brittle materials is still a topical issue today, as no comprehensive theory that is able to describe all the ways in which stress can occur without the introduction of special variables has yet been accepted. The numerical methods which are commonly used for the investigation of extensive problems that include fracture mechanics often need various extensions so that they are able to solve a given task successfully. The Smoothed Particle Hydrodynamics (SPH) method was not used in connection with quasi-brittle material failure for a long time due to the fact that it was not conceptually designed for the investigation of structural mechanics issues, but rather for hydrodynamics. However, in cases of high-speed stress, it is advantageous to use the SPH method because materials with structural strength behave in a similar way to fluids in such situations. Unfortunately, even this method suffers from false numerical dependencies which can influence the results of simulations in a negative manner. It can be concluded from executed tests that the initial regularity of the distribution of SPH particles plays an important role regardless of the investigated task. The contribution describes a test from the area of the simulation of dynamically loaded concrete structures using the SPH method. The primary subject of discussion is the influence of the initial distribution of particles on the results of simulations, as well as a possible solution to problems which arise due to the poor regularity of particle distribution. The simulations in question are compared with the experiment and results obtained via the Finite Element Method.

*Key-Words:* Smoothed particle hydrodynamics; support domain; nonlinear constitutive model; numerical fracture; concrete; dynamic loading.

## 1 Introduction

Many structures of high importance to society are designed using the principle of a skeleton, which is the main load-bearing part of the structure. The skeleton can be created as a series of spatially connected frames. Most frequently, structural steel or reinforced concrete is used as the building material for the primary load-bearing system. Each of these construction materials has its advantages and disadvantages - mainly during dynamic loading.

Thanks to the high strength of steel, structures can be designed very economically. This can result in structures within which thin profiles are predominant. Despite their possible high load-bearing capacity, such profiles are very prone to stability loss [1-3]. Indeed, whole frames can lose stability due to imperfections arising during production [4].

In the case of concrete structures, loss of stability is not necessarily a problem. This is frequently thanks to their robustness, which stems from the lower load-

bearing capacity of concrete in contrast with structural steel - the profiles used in structures must be more massive. However, negative aspects of the robustness of concrete start to appear when dynamic loading (e.g. seismicity) takes place. The occurrence of cracks is very frequent in the area of rigid frame joints. Of course, problems involving damage as a result of seismic activity also affect steel structures [5].

Loading does not necessarily have to be only of a natural character - quite the opposite. The question arises more and more frequently as to whether a structure should also be built to withstand intentional loading (e.g. plane crashes or explosions); see also [6-8]. It is obvious that deciding which specific material to choose is not a simple matter. Concrete (and its reinforced variants) is often chosen for its wide variability.

With regard to the frequent complexity of structures, concrete as a construction material and the type of loading itself, it is not possible to design a

structure without the execution of a simulation or numerical analysis. One of the most widely used numerical methods for the solution of complex issues is the Finite Element Method (FEM). In cases when the calculation also includes the aforementioned rigid frame joints, the FEM does not lead to correct results, particularly in cases of high-speed stress. Despite the availability of various material models of concrete [9, 10], which can be used to improve initial parameter optimization processes when needed [11], the acquisition of correct results can be very difficult when using the FEM method [12], or impossible in certain cases [13].

The answer to the question of how to successfully simulate a concrete frame joint exposed to high-speed stress can be found using the Smoothed Particle Hydrodynamics (SPH) method. This meshfree method differs from the FEM in that it operates without a physical mesh (or the physical connection of individual particles). It can deal with problems involving large deformations, including the resultant fragmentation of matter, without any major problems [14]. However, in cases when the distribution of SPH particles of the original geometry is not regular, the results do not correspond with those from experiments. The size of this problem is also influenced by the density of the discretization of the continuum.

In order to evaluate these dependencies, the contribution focuses on dynamic loading issues concerning concrete L-specimens which are simulated using the SPH method. In the executed simulations, the regularity of the distribution of SPH particles and its influence on the type of failure are primarily examined. Results from FEM simulations and experiments are used for comparison.

## 2 Essential formulation of the SPH

The formulation of the SPH method is often divided into two key steps. The first step is the *integral representation* of field functions, and the second is *particle approximation*. Assuming that the finite volume  $\Delta V_j$  is assigned to SPH particle  $j$ , the following relationship applies:

$$m_j = \Delta V_j \rho_j; \quad (1)$$

where  $m_j$  and  $\rho_j$  are the weight and density of particle  $j$ . The value of the monitored quantity  $f(\mathbf{x})$ , which is the product of integral representation and particle approximation operations, can thus be written as:

$$f(\mathbf{x}) \approx \sum_{j=1}^N \frac{m_j}{\rho_j} f(\mathbf{x}_j) W(\mathbf{x} - \mathbf{x}_j, h); \quad (2)$$

where  $W$  is the so-called smoothing function and  $h$  is the smoothing length defining the influence area of the smoothing function  $W$  – see Fig. 1

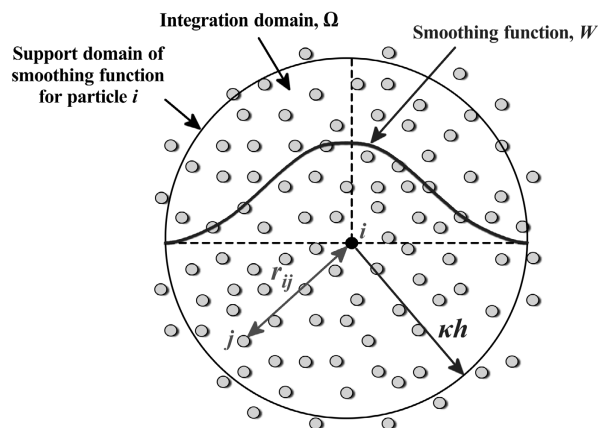


Fig. 1. Particle approximations using particles within the support domain of the smoothing function  $W$  for particle  $i$ .

### 2.1 Problem with the support domain

The extent of the support domain is defined according to Fig. 1 as the size of the generally variable parameter  $h$ , which is called the smoothing length. Parameter  $h$  can also be multiplied by constant  $\kappa$ . Particles which are inside the support domain attributable to particle  $i$  are called neighbouring particles. If the resultant value of the product  $\kappa h$  in each time step of the numerical simulation is the same, there can be the decrease in the number of neighbouring particles and thus also the decrease in the accuracy of the solution due the effect of excessive deformations (i.e. during the mutual divergence of the SPH particles). It is advisable to change the size of the support domain during the calculation in such a way that the number of neighbouring particles is constant.

There are many ways to dynamically develop  $h$  so that the number of neighbouring particles remains relatively constant. In 1989, Benz [15] suggested a method of developing the smoothing length. This method uses the time derivative of the smoothing function in terms of the continuity equation

$$\frac{dh}{dt} = -\frac{1}{d} h \frac{d\rho}{dt} = \frac{1}{d} h \nabla \cdot \mathbf{v} \quad (3)$$

where  $d$  is the number of dimensions and  $\nabla \cdot \mathbf{v}$  is the divergence of the flow velocity vector. This means

that the smoothing length increases when particles separate from each other and reduces when the concentration of particles is significant. It varies in order to keep the same number of particles in the neighbourhood. Equation (3) can be discretized using SPH approximations and calculated with other differential equations in parallel [16].

### 3 Experiment

In 2015, Ožbolt *et al.* [17] carried out experiments during which he controlled the displacement of L-shaped concrete specimens at different speeds. The aim of the experiments and subsequent numerical simulations was to discover the dependencies between the material strength and the loading speed.

Even though displacement control speeds of  $0.25 \text{ mms}^{-1}$  –  $2400 \text{ mms}^{-1}$  were tested in the experiment, this contribution only requires attention to be paid to the highest loading speed, i.e.  $2400 \text{ mms}^{-1}$ . Fig. 2 shows a diagram of the placement of concrete specimens from the executed experiment.

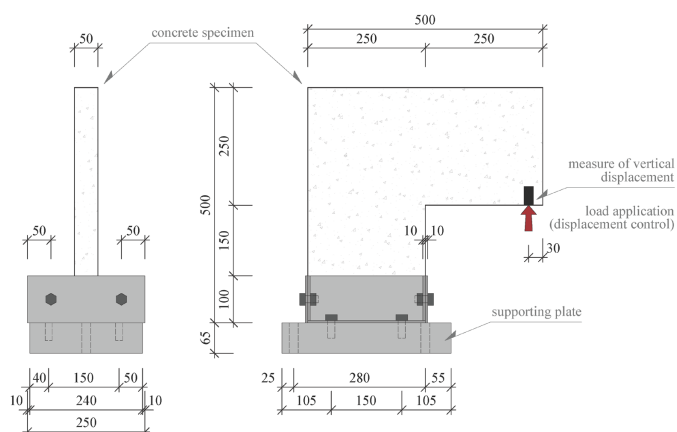


Fig. 2. Geometry and boundary conditions of the L-specimen (units in mm) [17].

Fig. 3 depicts type of failure at loading speed of  $2400 \text{ mms}^{-1}$ . In the experiment the type of failure changed due to the effect of loading speed [17]. With the change in loading speed, the resistance of the concrete specimen against deformation also changed, as did the measured maximum resistance strength – peak load. 127.73 kN was measured for a loading speed of  $2400 \text{ mms}^{-1}$ .

### 4 SPH and FEM simulations

The aim of carrying out numerical simulations using the SPH method was to achieve the values measured in the experiment (for a loading speed of  $2400 \text{ mms}^{-1}$ ). It was also used to obtain a corresponding failure

mode to that which can be seen in Fig. 3. Simulations were carried out also using the FEM method in order to check the SPH method's results. The initial geometry and placement were always the same (for all discretization variants), as can be seen in Fig. 2. Simulations were performed in the LS-DYNA program [18].

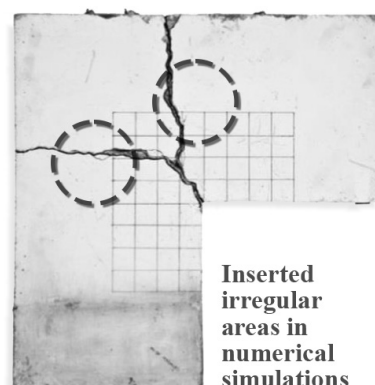


Fig. 3. L-specimen failure type for displacement loading speed of  $2400 \text{ ms}^{-1}$  [17].

#### 4.1 Material model of concrete

In the numerical simulations, only the concrete specimen without steel brackets was modelled. This was done to minimize possible numerical instabilities (e. g. contacts between steel and concrete). In this way, attention could be focused exclusively on the behaviour of the SPH method. The Continuous Surface Cap Model (CSCM) was chosen as the material model of concrete to be used [19, 20]. Table 1 shows the parameters used in the simulations.

Table 1

The material parameters for the CSCM model.

Mass density, $\rho_c$ ( $\text{kgm}^{-3}$ )	2210
Compressive strength, $f_c$ (MPa)	46.25
Tensile strength, $f_t$ (MPa)	3.12
Young's modulus, $E_c$ (GPa)	32.2
Poisson's ratio, $\nu_c$	0.18
Fracture energy, $G_F$ ( $\text{Jm}^{-2}$ )	58.56
Maximum aggregate size, $a_g$ (mm)	8

#### 4.2 From FEM to SPH

So that the results of the simulations of the FEM and SPH methods could be compared, FEM mesh was used as the basis for the creation of the SPH model. SPH particles were placed in the center of gravity of the FEM elements.

## 5 Simulation results

In the first results section, the functionality of the FEM and SPH methods is tested for a regular mesh with different division densities. In the second results section, an area with a rougher division is inserted into the original mesh (with the finest division). In addition, this area is intentionally placed at locations through which the crack is supposed to pass, see Fig. 3.

### 5.1. Regular mesh and density of spatial discretization

Discretization sizes of 16.66 mm, 10 mm and 6.25 mm were chosen for the FEM elements. In this way, division into 3, 5 and 8 elements were achieved along the thickness of the concrete specimen. As the SPH particles were created from FEM elements, the distances between them were also 16.66 mm, 10 mm and 6.25 mm. Figure 4 and Table 2 show the results for a regular FEM mesh and the distribution of SPH particles. The results correspond well with the experiments.

Table 2

The peak load for regular FEM mesh and SPH particle distribution.

Size	FEM	SPH	experiment
16.66 mm	123.07 kN	121.06 kN	
10.00 mm	126.78 kN	123.07 kN	127.73 kN
6.25 mm	130.08 kN	124.18 kN	

### 5.2. Irregular mesh and $\kappa$ parameter influence

In the second case, zones were inserted into the numerical model with element sizes of 6.25 mm where the size of the FEM mesh or the distance between the SPH particles was increased to 12.5 mm, i.e. 2x greater. With regard to this, an irregular zone of transition from size 6.25 mm to 12.5 mm was also created.

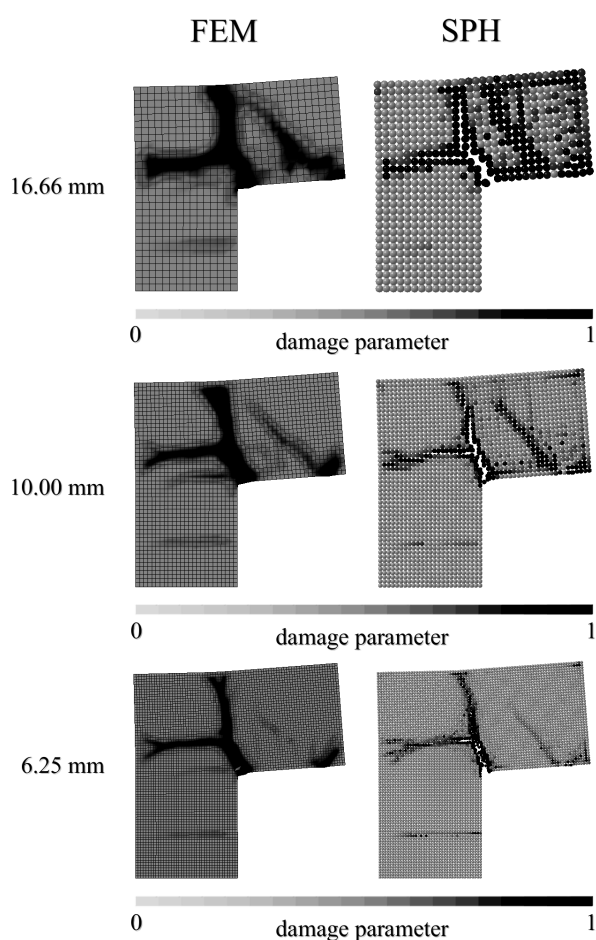


Fig. 4. Regular FEM mesh and SPH particle distribution results.

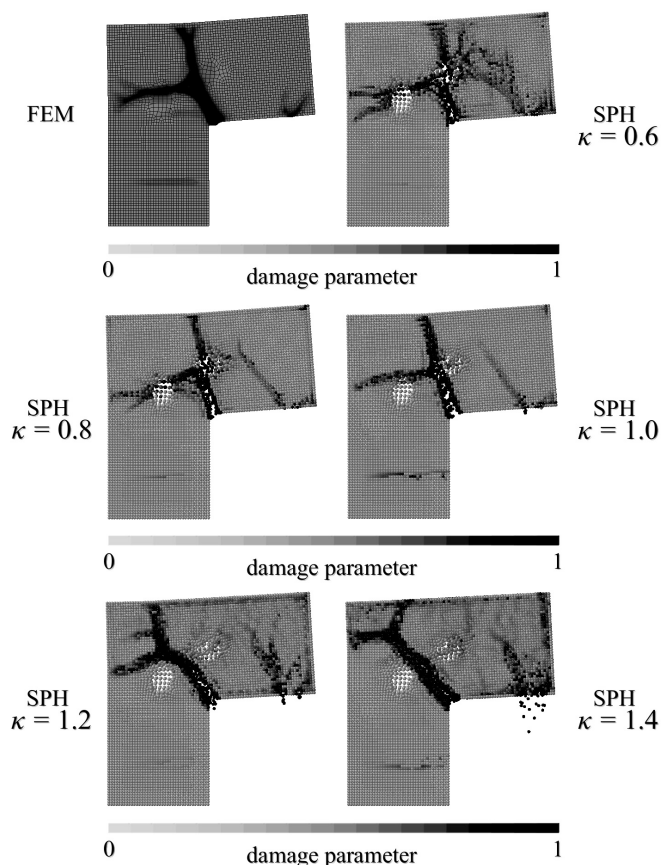


Fig. 5. Irregular FEM mesh and SPH particle distribution results.

Table 3

The peak load for irregular FEM mesh and SPH particle distribution.

Parameter $\kappa$	FEM	SPH	experiment
0.6		136.00 kN	
0.8		117.39 kN	
1.0	129.13 kN	100.03 kN	127.73 kN
1.2		76.38 kN	
1.4		44.68 kN	

Figure 5 and Table 3 show the results for an irregular FEM mesh and the distribution of SPH particles. Even though the results of the FEM simulation show that the inserted irregular area does not have a significant influence either on the size of the peak load or the shape of the failure, the result is strongly dependent on the selected parameter  $\kappa$  in the case of the SPH method, i.e. on the size of the support domain. In the case  $\kappa = 1$  it is obvious that the cracks avoid inserted areas with rougher division. Moreover, the measured strength does not correspond to the experiment. With increasing values of  $\kappa$ , the simulation results are increasingly different from the results of the experiment. The value  $\kappa < 1$  then shows a better correspondence between the simulation and the experiment. The optimum value of  $\kappa$  according to Table 3 appears to be  $\kappa \approx 0.7$ .

## 6 Conclusions

The regularity of the distribution of SPH particles plays a significant role in simulations which use the SPH method. In the cases of poor regularity and the use of quasi-brittle materials, unreal types of crack propagation can be expected. As a rule, cracks try to avoid areas where particle clusters occur. By choosing a suitable support domain size, results which correspond to those of experiments can be achieved. The size of the support domain can be reduced via parameter  $\kappa$ . It is apparent that the choice of  $\kappa < 1$  helps to reduce the size of the impact of poor regularity in the distribution of SPH particles.

## Acknowledgement

This outcome has been achieved with the financial support of project GACR 14-25320S "Aspects of the use of complex nonlinear material models" provided by the Czech Science Foundation and also with support of the project FAST-S-16-3718 "Advanced

numerical methods with complex material models" provided by the specific university research of Brno University of Technology.

## References:

- [1] Z. Kala, Sensitivity and Reliability Analyses of Lateral-torsional Buckling Resistance of Steel Beams, *Archives of Civil and Mechanical Engineering*, Vol.15, No.4, 2015, pp. 1098-1107.
- [2] Z. Kala, Reliability Analysis of the Lateral Torsional Buckling Resistance and the Ultimate Limit State of Steel Beams, *Journal of Civil Engineering and Management*, Vol.21, No.7, 2015, pp. 902-911.
- [3] J. Flodr, M. Krejsa, D. Mikolasek, J. Brozovsky, P. Parenica, Numerical modeling of a thin-walled profile with respect to the redistribution of bending moments, *Civil-Comp Proceedings*, Vol.108, 2015.
- [4] Z. Kala, Global Sensitivity Analysis in Stability Problems of Steel Frame Structures, *Journal of Civil Engineering and Management*, Vol.22, No.3, 2016, pp. 417-424.
- [5] J. Protivinsky, M. Krejsa, Reliability Assessment of the Dissipative Link in Steel Boiler Structure with Regard to Seismic Load, *4th International Conference on Materials Engineering for Advanced Technologies*, ICMEAT 2015, 2015, pp. 202-206.
- [6] J. Kralik, Safety of Nuclear Power Plants under the Aircraft Attack, *Applied Mechanics and Materials*, Vol.617, 2014, pp. 76-80.
- [7] J. Kralik, M. Baran, Numerical Analysis of the Exterior Explosion Effects on the Buildings with Barriers, *Applied Mechanics and Materials*, Vol.390, 2013, pp. 230-234.
- [8] J. Kralik, Optimal Design of NPP Containment Protection Against Fuel Container Drop, *Advanced Materials Research*, Vol.688, 2013, pp. 213-221.
- [9] P. Kral, J. Kala, P. Hradil, Verification of the Elasto-Plastic Behavior of Nonlinear Concrete Material Models, *International Journal of Mechanics*, Vol.10, 2016, pp. 175-181.
- [10] J. Kala, M. Husek, Useful Material Models of Concrete when High Speed Penetrating Fragments are Involved, *Proceedings of the 9th International Conference on Continuum Mechanics*, Vol.15, 2015, pp. 182-185.
- [11] F. Hokes, J. Kala, O. Krnavek, Nonlinear Numerical Simulation of a Fracture Test with Use of Optimization for Identification of

- Material Parameters, *International Journal of Mechanics*, Vol.10, 2016, pp. 159-166.
- [12] J. Kala, P. Hradil, M. Bajer, Reinforced concrete wall under shear load – Experimental and nonlinear simulation, *International Journal of Mechanics*, Vol.9, 2015, pp. 206-212.
- [13] J. Kala, M. Husek, High Speed Loading of Concrete Constructions with Transformation of Eroded Mass into the SPH, *International Journal of Mechanics*, Vol.10, 2016, pp. 145-150.
- [14] J. Kala, M. Husek, Improved Element Erosion Function for Concrete-Like Materials with the SPH Method, *Shock and Vibration*, Vol.2016, 2016, pp. 1-13.
- [15] W. Benz, Smoothed particle hydrodynamics: a review, *NATO Workshop*, Les, Arcs, France; 1989.
- [16] G. R. Liu, M. B. Liu, *Smoothed Particle Hydrodynamics: a meshfree particle method*, World Scientific Publishing Co. Pte. Ltd, 2003.
- [17] J. Ožbolt, N. Bede, A. Sharma, U. Mayer, Dynamic fracture of concrete L-specimen: Experimental and numerical study, *Engineering Fracture Mechanics*, Vol.148, 2015, pp. 27-41.
- [18] Livermore Software Technology Corporation (LSTC), *LS-DYNA Theory Manual*, LSTC, Livermore, California, USA, 2016.
- [19] Y. D. Murray, *User's manual for LS-DYNA concrete material model 159*, FHWA-HRT-05-062, 2007.
- [20] Y. D. Murray, A. Abu-Odeh, R. Bligh, *Evaluation of concrete material model 159*, FHWA-HRT-05-063, 2006.